Ha-Thanh Ngo, Thomas Bechtold*

Analysis of the Fibroin Solution State in Calcium Chloride/Water/Ethanol for Improved Understanding of the Regeneration Process

DOI: 10.5604/01.3001.0012.5174

Leopold-Franzens-University Innsbruck, Research Institute of Textile Chemistry and Textile Physics
Höchsterstraße 73 A-6850 Dornbirn
* e-mail: Thomas.Bechtold@uibk.ac.at

Abstract
Shaping of fibroin protein from Bombyx mori from calcium chloride/water/ethanol solution is of high interest for the manufacturing of biocompatible structures. Potentiometric titration experiments of the dissolved state permit new insight into the solution state of fibroin as a basis for improved regeneration. Titration experiments and infrared spectroscopy of the solution state support the model of an ion-rich hydration layer and interaction of the solvent with charged and polar groups of the fibroin, rather than through formation of defined calcium complexes. The potentiometric titration curves indicate the formation of calcium complexes at pH values above 9, most probably through involvement of basic amino acids and phenolic groups of tyrosine. After regeneration by the addition of methanol, the regenerated protein was characterised by FTIR, nitrogen and calcium analysis. The analysis of supernatants for their residual protein content indicated minor losses of protein, most probably low molecular weight proteins. The results contribute to an improved understanding of the solution state as a basis for larger scale regeneration, e.g. for the coating of textile fibres with regenerated fibroin.

Key words: *fibroin, calcium chloride, potentiometry, complex formation, regeneration, dissolution.*

Introduction

Silk fibres have been utilised for high level textiles for several thousands of years [1-3]. Through its particular mechanical and biomedical properties, silk fibroin is of high interest as biomaterial in tissue engineering as well as regenerative medicine [4-7]. A distinct advantage results from the high biocompatibility and processability into a wide range of shapes, e.g. fibres, sponges, films, hydrogels and composites [8-16]. Fibroin dissolves in a number of concentrated aqueous salt solutions, such as $CaCl_2$/water/ethanol (CWE) [12, 15, 17-20], $CaNO_3$/methanol/water [21] and LiBr [14, 20, 22-26], NaSCN [27]. Also ionic liquids e.g. 1-allyl-3-methylimidazolium chloride have been utilised to dissolve fibroin [28, 29].

During silk fibre formation in the silk glands of *Bombyx mori*, changes in the concentration of Ca^{2+} ions and shear stress are known to be relevant factors for the formation of an insoluble and partly crystalline fibroin structure [28]. Due to the tendency of the fibroin to aggregate and form micelles, the state of dissolved fibroin is rather complex. Instead of a coil arrangement of the chains, considerable protein-protein associations determine the solution behaviour of dissolved fibroin [30]. In the vast majority of techniques to regenerate fibroin from solution, dialysis is applied to reduce the salt concentration before fibroin regeneration is initiated [3]. The coagulation of fibroin is supported by non-solvents e.g. methanol and application of high shear rates. The presence of higher concentrations of calcium ions in the regenerates facilitates unwanted re-dissolution in water [18].

For larger scale application a simple regeneration process without the involvement of dialysis would be desirable, in an ideal case quantitative regeneration of the dissolved protein is achieved through direct destabilisation and coagulation of the dissolved fibroin [18, 31, 32]. However, this requires a more detailed understanding of the solution state of fibroin in CWE. The interaction of glutamate and aspartate amino side chains with calcium ions still is not fully understood.

Based on the concept of formation constants, potentiometric titrations can be used to analyse complex formation in solution [33]. To our knowledge, for the first time an adapted potentiometric titration technique was used for analysis of the solution state of sericine in CWE. The results allow us to distinguish between complex formation and non-specific interactions between the Ca^{2+}-ions and dissolved fibroin. In addition, the dissolved state was characterised by FTIR-ATR spectroscopy and viscometry. The fibroin regeneration process was initiated by direct addition of methanol. Regenerates were collected and characterised by FTIR and the Ca- and N- content. The results will contribute to an improved understanding of fibroin solution in CWE for better design of regeneration processes.

Experimental section

Material and chemicals

Raw silk hanks were obtained from the Nha Xa textile village, Ha Nam province, Vietnam. Na_2CO_3 (Merck, Darmstadt, Germany), $CaCl_2 \cdot 2H_2O$ (Fluka Chemie), ethanol (BVDA, Bureau voor Dactyloscopische Artikelen, Haarlem, Holland), methanol, $CaCO_3$ (Zeller GmbH, Hohenems, Austria), NaCl, H_3PO_4, NaOH, hydrochloric acid (Carl Roth GmbH), acetic acid and L-Aspartic acid (Sigma-Aldrich) were analytical grade chemicals. Coomassie Blue G-250 was supplied by Fluka (Buchs, CH).

Degumming

Prior to experimental work, silk yarns were conditioned at 65% RH and 20 °C for at least 24 hours. A weighed amount of silk was degummed in a solution of 5 g/l sodium carbonate Na_2CO_3 at boiling temperature (95 °C) for 30 min, 60 min and 90 min (LR = 1:100) to evaluate the influence of the boiling time [34]. Then samples were rinsed 5 times for 20 min with warm and cold deionised water and dried at ambient air temperature.

The dried degummed samples were conditioned for 24 hours at standard conditions (65% RH, 20 °C) to determine the mass loss (ML) in wt% during degumming see ***Equation (1)***.

$$ML = \frac{(m_1 - m_2)*100}{m_1} \quad (1)$$

Where m_1 and m_2 are the sample mass before and after degumming, respectively.

Staining experiments were used to assess the removal of sericin. Approximately 10 mg of silk were dyed in 10 ml of a solution containing 0.1 g of Direct Red 81 (DR81) in 10 ml of water (LR = 1:100) for 1 min. Samples were then rinsed with tap water. The degumming was assessed by the intensity of staining and quantified by measurement of CIELab coordinates. A spectrophotometer (Konica Minolta CM 3610d, Osaka, Japan) with d/8° geometry was used, and coordinates were calculated for D65 illumination. The L^* coordinate ranges from 0 (white) to 100 (black), where a positive a^* indicates a red colour and a negative value – a green colour. The b* axis describes the position on the yellow-blue axis.

Moisture content

For determination of the moisture content, weighed samples were dried for 4 hours at 60 °C, cooled down in a desiccator and then weighed again. For the open structure of the silk hanks used, a drying time of 4 h at 60 °C was sufficient to reach sorption equilibrium [35]. A temperature of 60 °C was used for drying to prevent any alteration due to thermal effects, which could occur at the standard drying temperature of 105 °C. The same temperature of 60 °C also was used for drying of the regenerates; thus a comparison of the weight of the initial sample and of the regenerates was possible. The moisture content MC_{60} (wt%) was calculated according to ***Equation (2)***.

$$MC_{60} = \frac{(A-B)*100}{B} \quad (2)$$

Where *A* is the weight of a wet sample, g and *B* that of a dried sample, g.

Preparation of fibroin solution

A calcium chloride/water/ethanol solution with a molar ratio of 1:8:2 (CWE) was used as a solvent for fibroin. To prepare such a solvent, 9.31 g of $CaCl_2 \cdot 2H_2O$ was dissolved in 6.85 g of deionised water, and then 5.84 g of ethanol was added. A weighed amount of degummed silk (0.2 g, 0.35 g, 0.5 g, 0.75 g, 1 g and 1.5 g) was immersed in 10 g of solvent to obtain fibroin solutions of different content (2.0, 3.4, 4.8, 7.0, 9.1, 13 wt%). The fibres were dissolved at 60 °C for 120 min to achieve complete dissolution. A mass of 0.3 g of 9.1 wt% solution was used to determine the protein content according to the Bradford method.

Regeneration of fibroin

A total volume of 70 ml of methanol was added to 10.7 g of the fibroin solution. The addition of methanol was performed stepwise in 4 portions of 15-20 ml. After each addition of methanol the solution was agitated for 15 min. Finally the solution was rested overnight to allow the regenerate to settle. Two independent repetitions were performed. The regenerated fibroin appeared as a sticky white substance, which adhered to the glass wall of the vessel (Regenerate 1) and partly remained dispersed in the liquid phase (Regenerate 2). The liquid phase was decanted off and filtered by a vacuum using cellulose-acetate filter paper. The solid residue in the vessel was washed with 10 ml of methanol, which was also filtered. The filtered residues were combined and dried to obtain Regenerate 2. A volume of 50 ml of deionised water was used to wash the fibroin collected in the vessel, which then was dried (Regenerate 1). All regenerates were dried at 60 °C for 4 h. A mass of 3 g of the methanol filtrate and of the water filtrate were both analysed for the residual protein content using the Bradford method.

Infrared spectroscopy

ATR-FTIR spectra were recorded using a Vector 22 FTIR spectrometer (Bruker, Karlsruhe Germany) equipped with a diamond crystal ATR stage. Spectra were recorded in 128 scans at a resolution of 1 cm^{-1} in the range of 4000-400 cm^{-1}. For FTIR analysis of the fibroin solution in CWE, the concentrated fibroin solution was directly placed on the ATR stage. Spectra for the dissolved fibroin were obtained by subtraction of the pure CWE absorbances from the fibroin-CWE spectrum. FTIR transmission spectra of solid samples were recorded via KBr pellets. A mass of 0.3-1 mg of the fibroin sample was added to 100 mg of pre-dried KBr (300 °C) and thoroughly ground.

Potentiometric titrations

Acid/base titrations of diluted solutions of dissolved fibroin were performed using a titroprocessor (Orion 960 Autochemistry System 960, Orion, Boston, MA) equipped with a pH electrode (Ross type electrode 81-02 Orion, USA). Titrations were performed starting from the pH value of the diluted solutions, either by the addition of 0.1 mol/l NaOH, or 0.1 mol/l HCl. A defined amount of 1.5 g of CWE, 1.5 g of fibroin solution (9.1 wt% fibroin in CWE) or 0.15 g of finely chopped degummed silk were filled up with deionised water to a volume of 50 ml, and 5 ml of 1 mol/l KCl was added to adjust the ionic strength. Titration was performed with fixed increments of 0.2 ml of titrant solution at a time interval of 5 seconds between the additions. Electrode calibration was performed by HCl/NaOH titrations and application of the Gran-function.

Viscometry

The viscosity of fibroin-CWE solutions was measured using an Ubbelohde capillary viscometer at 20 °C (type Ic, viscometer constant 0.029040 $mm^2\ s^{-2}$). Fibroin-CWE solutions of different concentration were prepared and analysed by the viscometer. Densities of the CWE and 1 wt% fibroin in CWE solution were determined by use of a pycnometer.

Protein analysis

Protein determination was performed by photometry according to the Bradford method [36]. The colour reagent was prepared by dissolving 100 mg of Coomassie Brillant Blue G-250 in 50 ml of 95 vol% ethanol, adding 100 ml of H_3PO_4 (85 wt%) and filling up to 1000 ml with deionised water. Before use, the solution was filtered through a paper filter (Whatman #1). The 9.1 wt% fibroin solution was used to prepare a calibration curve in the range of 0 µg and 90 µg fibroin. A volume of 100 µl of standard solution was mixed with 5 ml of the protein reagent. The absorbance was measured at 595 nm using a double beam spectrophotometer (Hitachi U-2000, Inula, Vienna) equipped with a 10 mm cuvette. For protein content analysis of the regeneration solutions, an exact amount of 0.3-3 g solution was placed in a 100 ml volumetric flask, diluted with 1 ml of 1 mol/l NaOH and filled to 100 ml with deionised water. Then a volume of 100 µl of this diluted solution was analysed with the Bradford method.

The composition of the sample solution was considered for preparation of the re-

spective blank solution depending on the fibroin solution to be analysed.

Calcium and nitrogen analysis

Calcium analysis of the samples was performed by means of an AAS (AAS spectrophotometer contrAA 300 HR-CS analytic jena, Jena Germany) according to EN ISO 7980:2000. The calibration curve was established using 0.25 g of pre-dried $CaCO_3$ (1 h at 180 °C), which was dissolved in 25 ml of 0.1 mol/l HCl and filled up to 100 ml with 0.1 mol/l HCl. Calibration solutions were prepared in the range of 0.5-5 mol/l Ca by taking an aliquot of the Ca-stock solution diluted by 0.1 mol/l HCl. A weighed amount of 50 mg of regenerated fibroin was extracted with 10 ml of 1 mol/l HCl at 60 °C for 1 hour. The solution was made up to 100 ml with deionised water and then filtered. The concentration of the extracts was adjusted with 0.5 mol/l HCl to obtain readings within the calibration range.

The nitrogen content of raw silk yarn, degummed silk and the regenerated fibroin fractions was determined using a nitrogen analyser. The measurement principle was based on the Dumas method (Elementar Rapid N III Nitrogen-Analyser, Elementar Analysensysteme GmbH, Hanan, Germany). L-Aspartic acid was used as a reference substance. A sample with a mass of 150 mg was cut into small pieces, wrapped in tin foil and pressed to a small tablet prior to combustion in the oven of an nitrogen analyser. The values given represent the mean values of at least two repetitions.

Results and discussion

FTIR-ATR analysis of fibroin in CWE

The silk was degummed in a solution of 5 g L^{-1} Na_2CO_3 at boiling temperature. The result of degumming was analysed by determination of the weight loss, CIE-Lab coordinates of samples stained with Direct Red 81 (DR 81) and by microscopy (data not given). A boiling time of 60 min was chosen for the degumming of silk. The moisture content of raw silk was determined to be 9.86 wt% and for degummed silk a value of 10.33 wt% was found, which is in agreement with literature [35]. In the range of 2.0-9.1 wt%, fibroin dissolution in CWE was completed within 30 min at 60 °C. For higher concentrations, e.g. 13 wt% fibroin, 4.5 hours were required for dissolution in CWE.

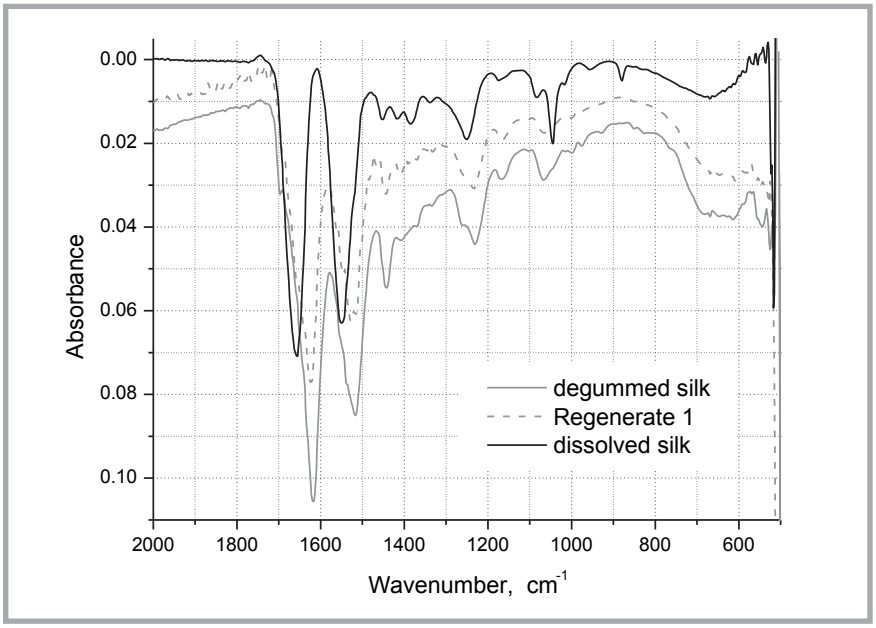

Figure 1. *FTIR spectra of degummed silk and Regenerate 1, FTIR-ATR analysis of 9.1 wt% fibroin-CWE solution.*

FTIR-ATR spectra of fibroin in CWE solution were obtained by subtraction of the CWE FTIR spectrum from the fibroin/CWE FTIR spectrum (***Figure 1***). As the ATR unit was equipped with a diamond crystal, the CWE solution could be placed directly on the ATR stage without undesired corrosion. In CWE the strong hydrogen bond interaction present in the β-pleated-sheet structure of the solid state is replaced by weak complex formation between fibroin and calcium ions and the formation of an α-helical structure. This assumption is in agreement with results reported on the calcium induced conformational changes of fibroin. Through the presence of calcium ions, existing hydrogen bond interactions and hydrophobic interactions are disrupted and the formation of α-helical structure initiated [37]. The characteristic vibrations of amide I (1680-1630 cm^{-1}) can be used to detect secondary conformational changes in the silk structure. Absorbance in the range of 1616 to 1637 cm^{-1} indicates β-sheet conformation, while a random coil structure is indicated by absorbance in the range of 1638 to 1655 cm^{-1}. The interval of 1656 to 1662 cm^{-1} is attributed to α-helical conformation, and absorbance in the region of 1663-1690 cm^{-1} is characteristic of the turns structure [37-40]. Compared to fibroin and regenerated fibroin, the fibroin solution in CWE exhibits a significant shift in amide I and amide II absorbances towards higher wavenumbers of 1655-1659 cm^{-1} for amide I and 1547-1553 cm^{-1} for amide II. A smaller shift is observed for amide III, which is detected near 1240 cm^{-1}. The peaks at 1040 cm^{-1} and 857 cm^{-1} can be explained by small differences in ethanol content in the CWE solution, which were not fully compensated during subtraction of the FTIR spectra.

Potentiometric titrations

In the presence of calcium, glutamate and aspartate residues in fibroin are suspected to contribute to stabilisation of α-helical conformation through modulation of the charge density [38]. At present it is still unclear if the formation of defined calcium fibroin complexes must be considered as the chemical principle contributing to fibroin dissolution in CWE. In cases where coordination complexes between glutamate and aspartate residues are formed, potentiometric titration of such complexes is a useful method to analyse complex stoichiometry and formation constants [33]. A schematic presentation of possible complex formation with the release of hydrogen ions is given in ***Equation (3)***.

$$[\text{Fibroin}] + n\,Ca^{2+} \rightleftharpoons [\text{Fibroin}\,H_{-2n}\,Ca_n] + 2n\,H^{+} \quad (3)$$

By the titration of a ligand solution alone and in the presence of the respective metal ion, the species distribution and formation constants of complexes can be determined; however, a number of assumptions have to be considered which will define limits for a detailed interpretation.

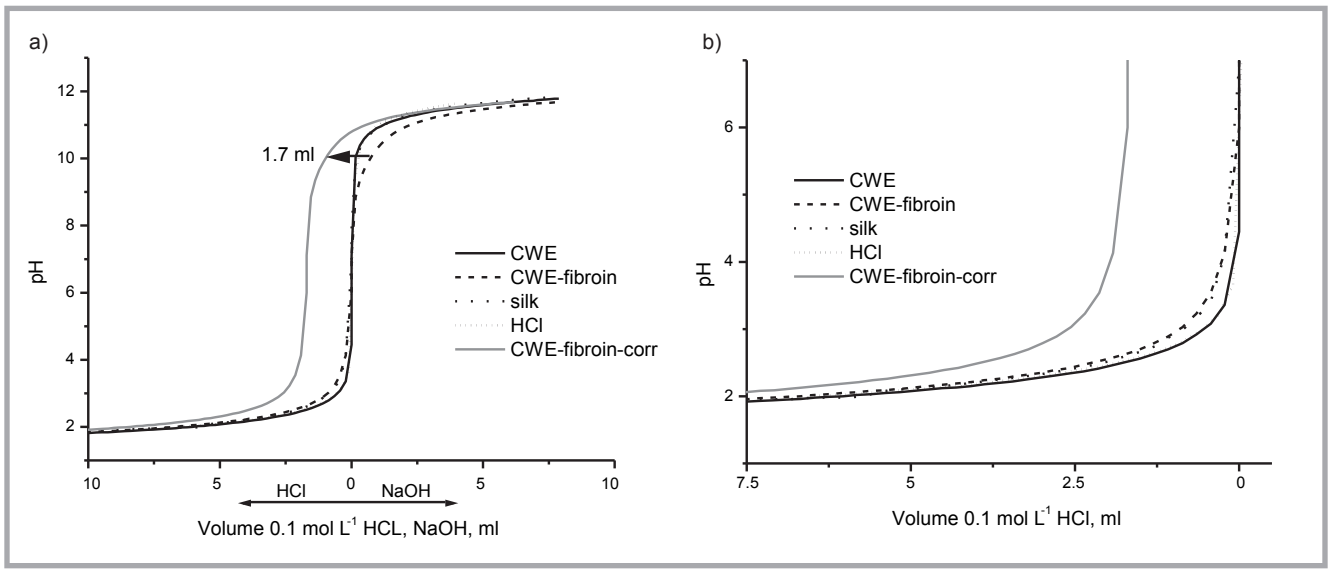

Figure 2. *a) Combined titrations curves of CWE solution, fibroin in CWE solution and silk powder in water, and titration curve of HCl (0.1 mol L^{-1}) with NaOH (0.1 mol L^{-1}); b) magnified sector of titration curves.*

- A defined stoichiometry is required to establish an accurate reaction model. Fibroin consists of different amino acids, thus a high number of different binding sites is available within a single protein chain.
- Qualified analysis requires titration of rather diluted solutions of ligand and metal. Fibroin-CWE solution is formed in concentrated $CaCl_2$-ethanol solutions only.
- The titration of pure ligand (fibroin) in this case is possible only in the form of insoluble dispersed silk fibres, thus accessibility of the fibres could have an influence on the shape of the titration curve.

Irrespective of these assumptions, the presence of defined coordination complexes should lead to an additional potential break in the potentiometric titration curve.

For determination of formation constants, potentiometric titration analysis is started either from an acid or alkaline pH. As such conditions would alter the solution state of the fibroin before the titration, two independent experiments were performed, each starting with the diluted fibroin-CWE solution at pH 6.68-7.12, which was then titrated either by the addition of acid or alkali. The two titration curves were then combined to obtain an overall potentiometric curve. For comparison, diluted CWE solution and powdered degummed fibroin were analysed (***Figure 2***).

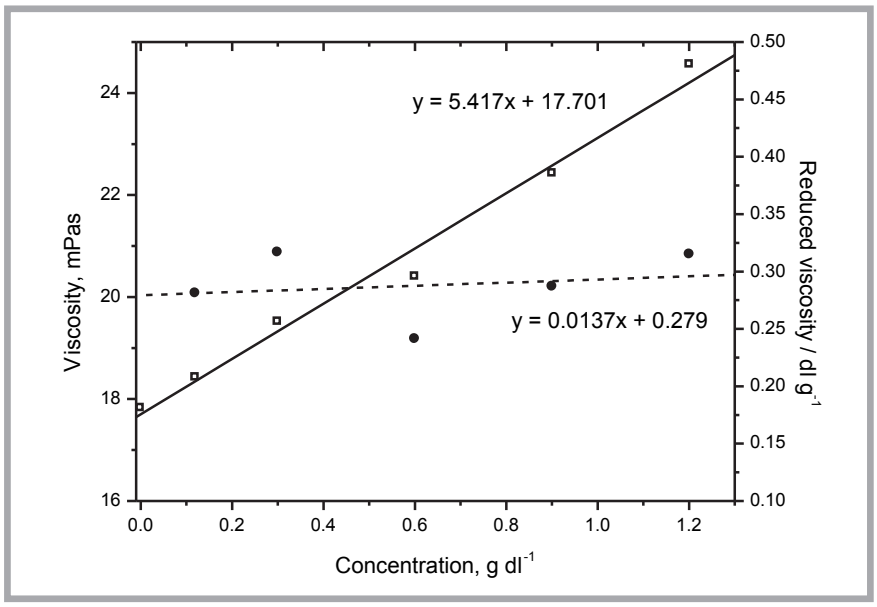

Figure 3*. Viscosity (▫) and reduced viscosity (•) of fibroin in CWE as function of the concentration.*

The curve for the titration of CWE solution can be overlapped with the direct titration of HCl with NaOH without significant differences, thus indicating that an aqueous $CaCl_2$-ethanol mixture does not generate a significant consumption of acid or base.

Experiments performed in the presence of dissolved fibroin or silk fibres exhibit a slight change in titration curves between pH 2.5 and pH 4 when compared to titrations of HCl or CWE. This can be explained by the neutralisation of carboxylic groups from acidic amino acid glutamate (2.0 %wt) and aspartate (2.0 %wt) [41-43].

Between pH 2 and 7 no indication of complex formation between Ca^{2+} ions of CWE and acidic groups of fibroin is given by the potentiometric titration curves. In this pH range carboxylic side groups (aspartic acid 2.0 wt%; glutamic acid 2.03 wt%) fully dissociate [38-40]. In the case of a distinct complex between calcium and carboxylic groups of amino acids being formed, an additional potential break should appear in the titration curves near to the pH range where complex formation occurs. The absence of such a buffer plateau supports the assumption that the dissolution of fibroin in CWE does not involve the formation of distinct Ca^{2+}-fibroin complexes [9].

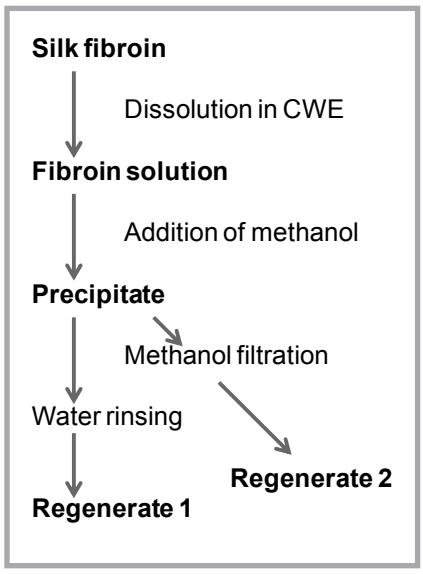

Figure 4. *Scheme of the regeneration process.*

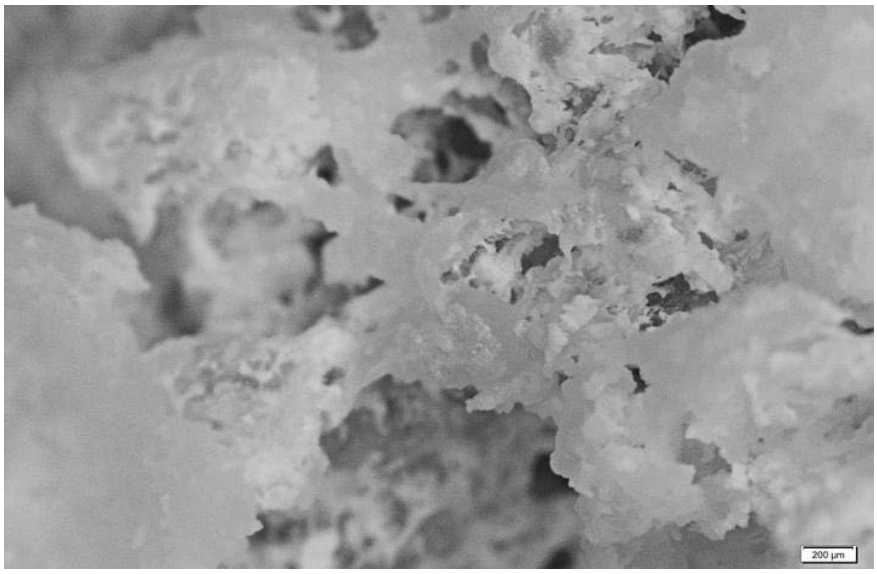

Figure 5. *Photomicrograph of Regenerate 1 (scale bar 200 µm).*

The major effect of fibroin dissolution in CWE is thus based on the cleavage of salt bridges and hydrogen bridges at the high ionic strength of the solvent. FTIR-ATR spectra of the fibroin solution in CWE are in agreement with the proposed presence of rather non-specific interactions between the CWE and polar groups of fibroin.

A distinct change in alkali consumption between CWE and fibroin-CWE can be observed in the pH range 9-11, where neutralisation of the phenolic groups of tyrosine (13.2 wt% in fibroin) and deprotonation of amino groups of basic amino acids (arginine, lysine, histidine) are expected to occur [40]. The consumption of alkali can be estimated by shifting the fibroin-CWE titration curve to overlap with the titration curve of CWE at pH 11, which then indicates a difference in alkali consumption of 1.7 ml. This corresponds to an alkali consumption of 0.17 mmoles for a titration of 1.5 g of 9.1 wt% fibroin CWE solution, which is due to complex formation between calcium ions and dissolved fibroin above pH 9. At this high pH the phenolic groups of tyrosine and amino groups of basic amino acids can participate in calcium complex formation. The content of such amino acids in fibroin is sufficient to explain the alkali consumption through formation of Ca^{2+}-amino acid complexes observed.

Viscometry of fibroin solution in CWE

The intrinsic viscosity of the fibroin solution was determined as 17.7 mPas, which is in accordance to the results determined for LiBr and CWE [22,44]. ***Figure 3*** presents the viscosity and reduced viscosity as a function of fibroin concentration. A concentration dependent increase in the viscosity of CWE was observed, and an intrinsic viscosity of 0.279 dl g^{-1} was determined. The low dependency of reduced viscosity on fibroin concentration suggests that no increase in the association or formation of protein aggregates occurs within the concentration range investigated, which is in agreement with the results from potentiometric titrations and FTIR-ATR measurements.

Regeneration experiments

A general scheme of the process is given in ***Figure 4***. The direct addition of methanol to 9.1 wt% fibroin-CWE solution leads to protein coagulation and precipitation of a white sticky substance, which settles and adheres to the glass walls of the vessel (Regenerate 1). Dispersed regenerate was collected by filtration (Regenerate 2). A photomicrograph of the dried coagulate is shown in ***Figure 5***. From the input of fibroin and the weight of regenerated protein, an overall mass balance for the regeneration process was established (***Table 1***). Calcium analysis of the regenerated fibroin samples indicated that Regenerate 1 contained between 10 wt% and 15 wt% of its calcium weight, which is in agreement with the overall increase in the mass of regenerate collected. The presence of approximately 15-20 % of $CaCO_3$ % in the regenerated fibroin explains the experimental yield of 110-121% in total, shown in ***Table 1***. The precipitation of aspartate and glutamate in the form of their corresponding calcium salts would lead to 1.3 %wt bound Ca, which thus indicates the presence of substantial amounts of co-precipitated, weakly bound calcium chloride.

The Bradford method permits determination of the protein concentration in

Table 1. *Mass balances for fibroin dissolution and regeneration (2 independent experiments) and overall yield of regenerated fibroin.*

Experiment	Dissolved fibroin mass	Regenerate 1 mass	Ca^{2+} content	Regenerate 2 mass	Yield
No.	g	g	%	g	%
1	1.04	1.20	15.7	0.0597	121
2	1.01	1.04	9.4	0.0752	110

Table 2. *Analysis of residual protein content in supernatant obtained during fibroin regeneration, and the amount of protein detected in % of the initial amount used.*

Regenerate	Sample mass, g	Absorbance	Protein, µg	Total protein, %
9.1 wt% fibroin/CWE	0.3	0.12	27.3	100
Methanol solution	3	0.04	11.2	30.0
Aqueous solution	3	0.02	4.4	7.4

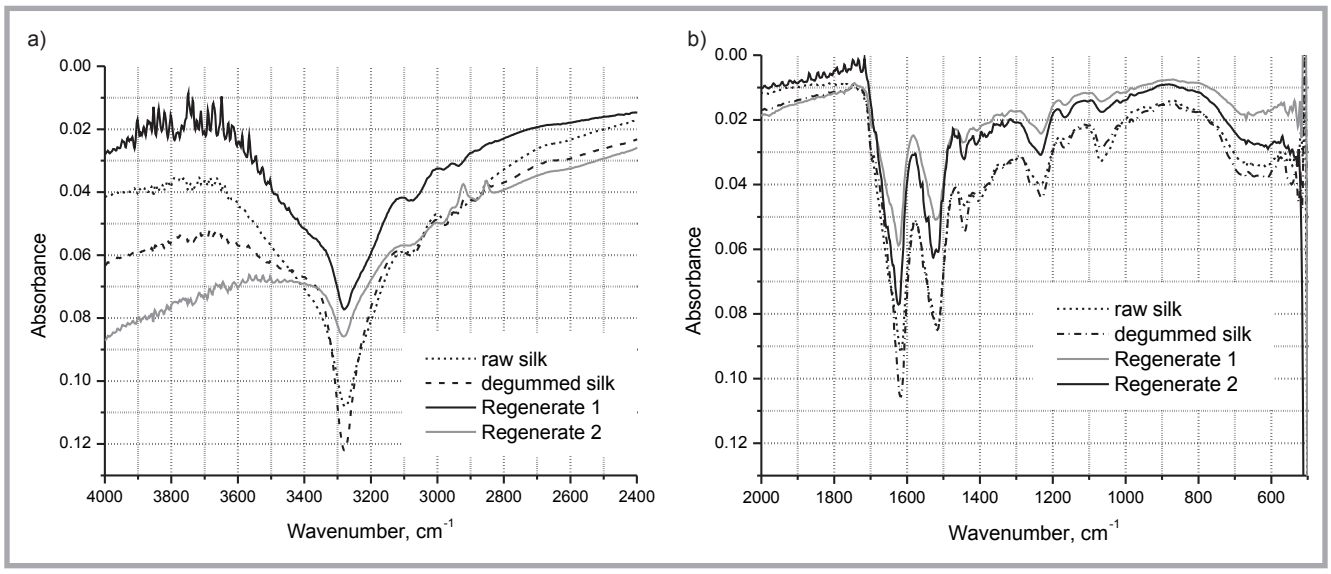

***Figure 6**. FTIR analysis of raw silk, degummed silk, and Regenerates 1 & 2.*

Table 3 *Analysis of nitrogen content in silk samples and regenerated silk.*

Sample	N-content (wt% ± s.d.)
Raw silk	16.8 ± 0.01
Degummed silk	17.4 ± 0.11
Regenerate 1	14.9 ± 1.0
Fibroin	18.3 [47]
Sericin	16.5 [47]

solution (***Table 2***). Coomassie Brilliant Blue G250 forms complexes with cationic and apolar side groups of the protein, which leads to an increase in absorbance at 595 nm and permits determination of the protein concentration. Noticeable non-linearity of the calibration curve was observed, which can be explained by the limited solubility of fibroin in the diluted protein assay and by the formation of protein aggregates.

Substantial amounts of protein were seen to remain dissolved in the methanol solution, which can be explained by protein fractionation during the methanol regeneration and possible accumulation of low molecular weight proteins. Fibroin from *Bombyx mori* consists of three different protein components, the high molecular mass H-chain, which is bound to the lower molecular mass L-chain through disulfide bonds and the smaller P25 protein [45, 46]. When the fibroin is dissolved in CWE, separation of non-covalently bound proteins is expected to occur. Low molecular weight proteins are supposed to remain dissolved in the regeneration solution, thus leading to a corresponding response in accordance with the Bradford method.

Regenerate 1 was also characterised by determination of the N-content and by FTIR-spectroscopy (***Table 3***, ***Figure 6***). The increase in N-content with degumming is in accordance with the results given in literature [47]. The removal of sericin leads to an increase in N-content to 17.4 wt%. In Regenerate 1 the N-content is reduced, which can be explained by the presence of significant amounts of calcium of up to 10-20 wt%.

For raw silk, FTIR absorption was observed at a wavenumber of 1400 cm^{-1}, which disappeared after degumming due to the removal of sericine. No significant differences in the FTIR spectra were detected between degummed silk and regenerated fibroin, which indicates that the CWE treatment did not lead to substantial chemical modification in the primary structure of fibroin. A possible explanation for Ca-content in the regenerated fibroin could be the presence of $CaCO_3$ formed during the regeneration. The presence of $CaCO_3$ should be detectable in the FTIR spectra through characteristic absorbance at 1440 cm^{-1} and 873 cm^{-1}, which was not visible in the spectra of the regenerated fibroin [48]. This supports the model of a retarded release of weakly bound $CaCl_2$ during the regeneration procedure. The addition of methanol as a non-solvent first leads to the precipitation of Ca-containing fibroin coagulates, which partially persist during the following aqueous rinsing steps. This result is in agreement with experiments published for fibroin regeneration from calcium nitrate – methanol solutions, where calcium containing domains were identified in regenerated fibroin films [17].

Conclusions

The FTIR-ATR analysis and potentiometric titration of the fibroin-CWE solution indicate that dissolution occurs through formation of an ion-rich hydration layer and interaction of the concentrated calcium solution with charged and highly polar groups of the fibroin, rather than through formation of well-defined Ca^{2+}-complexes. This model is also supported by the low complex formation constants published for Ca^{2+}-complexes with major silk constituents, e.g. glycine, alanine, tyrosine and serine [49]. In fibroin the share of amino acids with carboxylic side groups or basic amino groups, which could form more stable Ca^{2+} complexes, is not sufficient to explain dissolution in CWE through the formation of defined complexes [50]. The high calcium concentration in CWE favours the formation of weak complexes. Charge repulsion results from the binding of calcium to negatively charged amino acids e.g. glutamate and aspartate, which contributes to stabilisation of the dissolved state [38]. A schematic representation of the weak interactions between Ca^{2+} ions and the fibroin protein chain is shown in ***Figure 7***. The structure of weak complexes was proposed as opposed to the well-known Ca^{2+} complexes e.g. a calcium complex with ethylenediaminetetraacetic acid [51]. The inclusion of NH-groups of the peptide chain allows formation of five-membered chelate structures.

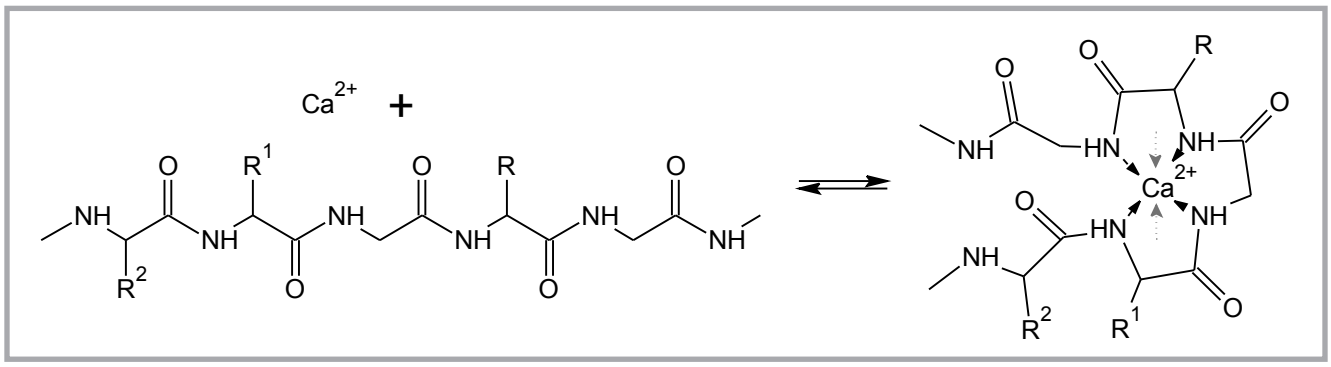

***Figure 7**. Schematic presentation of Ca^{2+} interaction with fibroin in CWE*

The presence of defined calcium complexes of fibroin in CWE would permit coagulation and regeneration through a change in solution pH, e.g. towards the region of lower complex stability. From literature it is known that a reduction in pH supports aggregation and fibroin regeneration; however, it is not feasible to achieve an efficient regeneration [25]. The dilution of fibroin-CWE with water destabilised the ion-rich hydration layer, but coagulation and regeneration proceed only very slowly and incompletely.

The presence of high amounts of calcium in the regenerated fibroin explains the undesirable water solubility of freshly precipitated fibroin. Sufficient time has to be given during the methanol coagulation before rinsing with water.

Based on the gravimetric analysis and the analysis of protein losses in the solution, the recovery of fibroin proteins can be estimated to be above 90 wt%. Considerable protein content was found in the methanol supernatant, which can be explained by protein fractionation and accumulation of low molecular weight proteins. An almost complete regeneration is a pre-requisite for a technique to be useful in fibroin shaping processes, as substantial losses would prevent cost efficient application in larger scale processes.

In the next step, the technique presented will be modified to regenerate fibroin as a coating for fibrous substrates, with the aim of forming hybrid fibres e.g. with a synthetic polymer core and fibroin surface.

Acknowledgements

The authors wish to thank OeAD (Austrian agency for international mobility and cooperation in education, science and research) for providing a PhD-scholarship to Ha Thanh Ngo. They are also grateful to Dr. Barnaby Caven for technical and language proofreading.

References

1. Padaki N V, Das B, Basu A. *Advances in Silk Science and Technology*, Chapter 1 – Advances in understanding the properties of silk, in Adv. Silk Sci. Technol., (Ed.: A. Basu), Woodhead Publishing, Cambridge, 2015, Ch. 1, p. 3.
2. Altman G H, Diaz F, Jakuba C, Calabro T, Horan R L, Chen J, Lu H, Richmond J, Kaplan D L. Silk-based biomaterials. *Biomaterials* 2003; 24: 401-416.
3. Vepari C, Kaplan D L. Silk as a biomaterial. *Prog. Polym. Sci*. 2007; 32: 991-1007.
4. Pereira R F P, Silva M M, de Zea Bermudez V. Bombyx mori Silk Fibers: An Outstanding Family of Materials. *Macromol. Mater. Eng*. 2015; 300: 1171-1198.
5. Zhao W, Jin X, Cong Y, Liu Y, Fu J. Degradable natural polymer hydrogels for articular cartilage tissue engineering. *J. Chem. Technol. Biotechnol*. 2013; 88: 327-339.
6. Zhang Y Q, Tao M L, De Shen W, Mao J P, Chen Y H. Synthesis of silk sericin peptides–Lasparaginase bioconjugates and their characterization. *J. Chem. Technol. Biotechnol.* 2006; 81: 136-145.
7. Silva N H C S, Vilela C, Marrucho I M, Freire C S R, Pascoal Neto C, Silvestre A J D. Protein-based materials: from sources to innovative sustainable materials for biomedical Applications. *J. Mater. Chem. B* 2014; 2: 3715-3740.
8. Abdel-Naby W, Lawrence B D. *Processing of silk biomaterials.* in Adv. Silk Sci. Technol., (Ed.: A. Basu), Woodhead Publishing, Cambridge 2015, Ch. 9, p.171.
9. Hardy J G, Römer L M, Scheibel T R. Polymeric materials based on silk proteins. *Polymer (Guildf).* 2008; 49: 4309-4327.
10. Teimouri A, Ebrahimi R, Emadi R, Beni B H, Chermahini A N. Nano-composite of silk fibroin–chitosan/Nano ZrO_2 for tissue engineering applications: Fabrication and morphology. *Int. J. Biol. Macromol*. 2015; 76: 292-302.
11. Samal S K, Kaplan D L, Chiellini E. Ultrasound sonification effects on silk fibroin protein. *Macromol. Mater. Eng*. 2013; 298: 1201-1208.
12. Srisuwan Y, Srihanam P, Baimark Y. Preparation of silk fibroin microspheres and its application to protein adsorption. *J. Macromol. Sci., Part A: Pure and Appl. Chem.* 2009; 46: 521-525.
13. Yetiskin B, Okay O. High-strength silk fibroin scaffolds with anisotropic mechanical properties. *Polymer* 2017; 112: 61-70.
14. Bie S, Ming J, Zhou Y, Zhong T, Zhang F, Zuo B. Rapid formation of flexible silk fibroin gel-like films. *J. Appl. Polym. Sci*. 2015; 132: 41842.
15. Silva M F, De Moraes M A, Nogueira G M, Rodas A C D, Higa O Z, Beppu M M. Glycerin and ethanol as additives on silk fibroin films: Insoluble and malleable films. *J. Appl. Polym. Sci*. 2013;128: 115-122.
16. Zuo L, Zhang F, Gao B, Zuo B. Fabrication of Electrical Conductivity and Reinforced Electrospun Silk Nanofibers with MWNTs. *FIBRES & TEXTILES in Eastern Europe* 2017; 25, 3(123): 40-44. DOI: 10.5604/01.3001.0010.1687.
17. Liang C X, Hirabayashi K. Improvements of the physical properties of fibroin membranes with sodium alginate. *J. Appl. Polym. Sci*. 1992; 45: 1937-1943.
18. Ha S W, Park Y H, Hudson S M. Dissolution of Bombyx mori silk fibroin in the calcium nitrate tetrahydrate-methanol system and aspects of wet spinning of fibroin solution. *Biomacromolecules*, 2003; 4: 488-496.
19. Kawahara Y, Furukawa K, Yamamoto T. Self-Expansion Behavior of Silk Fibroin Film. *Macromol. Mater. Eng*. 2006; 291: 458-462.
20. Ajisawa A. Dissolution of silk fibroin with calciumchloride/ethanol aqueous solution. *J.Seric. Sci. Jpn* 1998; 67: 91-94.
21. Mathur A B, Tonelli A, Rathke T, Hudson S. The dissolution and characterisation of Bombyx Mori Silk Fibroin in Calcium Nitrate-Methanol Solution and the Regeneration of Films. *Biopolymers* 1997; 42: 61-74.
22. Matsumoto A, Lindsay A, Abedian B, Kaplan D L. Silk Fibroin Solution Properties Related to Assembly and Structure. *Macromol. Biosci*. 2008; 8: 1006-1018.
23. Liu Y, Liu H, Qian J, Deng J, Yu T. Immobilization of Glucose Oxidase in the Regenerated Silk Fibroin Membrane: Characterization of the Membrane Structure

and Its Application to an Amperometric Glucose Sensor Employing Ferrocene as Electron Shuttle. *J. Chem. Technol. Biotechnol.* 1995; 64: 269-276.
24. Zuo B, Liu L, Wu Z. Effect on properties of regenerated silk fibroin fiber coagulated with aqueous methanol/ethanol. *J. Appl. Polym. Sci*. 2007; 106: 53-59.
25. Sun Y, Shao Z, Ma M, Hu P, Liu Y, Yu T. Acrylic Polymer – Silk Fibroin Blend Fibres. *J. Appl. Polym. Sci*. 1997; 65:959-966.
26. Strobin G, Wawro D, Stęplewski W, Ciechańska D, Jóźwicka J, Sobczak S, Haga A. Formation of Cellulose/Silk-Fibroin Blended Fibres. *FIBRES & TEXTILES in Eastern Europe* 2006; 14, 4 (58): 32-35.
27. Strobin G, Ciechańska D, Wawro D, Stęplewski W, Jóźwicka J, Sobczak S, Haga A. Chitosan Fibres Modified by Fibroin. *FIBRES & TEXTILES in Eastern Europe* 2007; 15, 5-6(64-65): 146-148.
28. Wang Q, Chen Q, Yang Y, Shao Z. Effect of Various Dissolution Systems on the Molecular Weight of Regenerated Silk Fibroin. *Biomacromolecules* 2013; 14: 285-289.
29. Kuzmina OG, Sashina ES, Novoselov NP, Zaborski M. Blends of Cellulose and Silk Fibroin in 1-buthyl-3-methylimidazolium chloride Based Solutions. *FIBRES & TEXTILES in Eastern Europe* 2009; 17, 6(77): 36-39.
30. Kaplan D L, Mello C M, Arcidiacono S, Fossey S, Senecal K, Muller W. in *Protein-Based Mater*., (Eds.: K. McGrath, David. Kaplan), Birkhauser Boston, Boston, USA 1997, Ch. 4, p. 114.
31. Ngo H T, Bechtold T. Sorption behaviour of reactive dyed labelled fibroin on fibrous substrates. *J. Appl. Polym. Sci*. 2016; 133(35): DOI: 10.1002/APP 43880.
32. Ngo H T, Bechtold T. Surface modification of textile material through deposition of regenerated silk fibroin. *J. Appl. Polym. Sci*. 2017; DOI: 10.1002/app.45098.
33. Arthur R J M, Martell E. *Determination and Use of Stability Constants.* VCH Publishers, New York/ Weinheim 1992.
34. Wang F, Cao T T, Zhang Y Q. Effect of silk protein surfactant on silk degumming and its properties. *Mater. Sci. Eng. C* 2015; 55: 131-136.
35. Reumann R D., *Pruefverfahren in der Textil- und Bekleidungsindustrie*, Springer, Berlin, Germany 2000.
36. Bradford M M. A rapid and sensitive method for the quantitation of microgram quantities of protein utilizing the principle of protein-dye binding. *Anal. Biochem*. 1976; 72: 248-254.
37. Dubey P, Murab S, Karmakar S, Chowdhury P K, Ghosh S. Modulation of self-assembly process of fibroin: an insight for regulating the conformation of silk biomaterials. *Biomacromolecules* 2015; 16(12): 3936-3944.
38. Lu Q, Zhang B, Li M, Zuo B, Kaplan D L, Huang Y, Zhu H. Degradation mechanism and control of silk fibroin. *Biomacromolecules* 2011; 12: 1080-1086.
39. Hu X, Kaplan D, Cebe P. Determining Beta-Sheet Crystallinity in Fibrous Proteins by Thermal Analysis and Infrared Spectroscopy. *Macromolecules* 2006; 39(18): 6161-6170.
40. Zhang C, Song D, Lu Q, Hu X, Kaplan D L, Zhu H. Flexibility Regeneration of Silk Fibroin in Vitro. *Biomacromolecules* 2012; 13(7): 2148-2153.
41. Rath H. *Lehrbuch Der Textilchemie*, Springer-Verlag Berlin Heidelberg, 1972.
42. Vickery H B, Block R J. The basic amino acids of silk fibroin. The determination of basic amino acids yielded by proteins, *J. Biol. Chem*. 1931; 93: 105-112.
43. Corfield M C, Howitt F O, Robson A. Basic Amino-acids of Silk Fibroin, *Nature* 1954; 174: 603-604.
44. Wang H-Y, Zhang Y-Q. Effect of regeneration of liquid silk fibroin on its structure and characterization. *Soft Matter* 2013; 9:138-145.
45. Tanaka K, Inoue S, Mizuno S. Hydrophobic interaction of P25, containing Asn-linked oligosaccharide chains, with the HL complex of silk fibroin produced by Bombyx mori. *Insect Biochem. Mol. Biol*. 1999; 29: 269-276.
46. Kundu B, Rajkhowa R, Kundu S C, Wang X. Silk fibroin biomaterials for tissue regenerations. *Adv. Drug Deliv. Rev*. 2013; 65: 457-470.
47. Whewell C S. *Fibres, Animal, Silk*. Vol 5., J. F. Thorpe, M. A. Whiteley, in Thorpe's Dict. Appl. Chem., 4th Edition, New York 1941, p. 87.
48. "Calcium carbonate (precipitated)," http://webbook.nist.gov/cgi/cbook.cgi?ID=C471341&Mask=80
49. Rey F, Antelo J M, Arc F, Penedo FJ. Equilibrium Constants of Metal Amino Acid Complexes. *Polyhedron* 1990; 9/5: 665468.
50. Fox S, Bu1sching I, Barklage W, Strasdeit H. Coordination of Biologically Important r-Amino Acids to Calcium (II) at High pH: Insights from Crystal Structures of Calcium a-Aminocarboxylates. *Inorg. Chem*. 2007; 46: 818-824.
51. https://www.britannica.com/science/coordination-compound/Ligands-and-chelates, accessed 2016.07.03.

Received 06.04.2017 Reviewed 28.08.2018